

Extravasation of Poly(amidoamine) (PAMAM) Dendrimers Across Microvascular Network Endothelium

Mohamed El-Sayed,¹ Mohammad F. Kiani,²
Mike D. Naimark,² Ahmed H. Hikal,^{3,4} and
Hamidreza Ghandehari^{1,5}

Received August 29, 2000; Accepted September 25, 2000

Purpose. To study the influence of a controlled incremental increase in size and molecular weight of a series of poly(amidoamine) (PAMAM) dendrimers on their extravasation across the microvascular network endothelium.

Methods. A series of PAMAM dendrimers (generations 0–4) were fluorescently labeled using fluorescein isothiocyanate (FITC). Purification and fractionation of the fluorescently labeled polymers were done using size exclusion chromatography. The hamster cremaster muscle preparation was used as an *in vivo* model to study the extravasation process of the fluorescently labeled polymers. The extravasation process was visualized and recorded using intravital microscopy techniques. Analysis of the recorded experiments was done using Metamorph Imaging System. Extravasation of the fluorescently labeled polymers is reported in terms of their extravasation time (τ), i.e., the time needed for the fluorescence intensity in the interstitial tissue to reach 90% of the fluorescence intensity in the neighboring microvessels.

Results. Extravasation time (τ) describes the rate of microvascular extravasation of polymeric drug carriers across the microvascular endothelium into the interstitial tissue. Extravasation time (τ) of the studied PAMAM dendrimers showed size and molecular weight dependence. An increase in size and/or molecular weight of PAMAM dendrimers resulted in a corresponding exponential increase in the extravasation time (τ).

Conclusions. Extravasation of PAMAM dendrimers across the microvascular endothelium showed size and molecular weight dependence. Results suggest that in addition to size and molecular weight, other physicochemical properties of polymeric drug carriers such as molecular geometry and charge may influence their microvascular extravasation. Systematic studies of the influence of the physicochemical properties of polymeric drug carriers on their microvascular extravasation will aid in the design of novel macromolecular drug carriers with controlled extravasation profiles.

KEY WORDS: poly(amidoamine) dendrimers; poly(ethylene glycol); microvascular extravasation; endothelial barrier; intravital microscopy; drug delivery.

¹ Department of Pharmaceutical Sciences, School of Pharmacy, University of Maryland at Baltimore, Baltimore, Maryland.

² School of Biomedical Engineering and Department of Radiation Oncology, University of Tennessee Health Sciences Center, Memphis, Tennessee.

³ Department of Pharmaceutics and the National Center for Natural Products Research, School of Pharmacy, University of Mississippi, University, Mississippi.

⁴ Present address: Department of Research and Development, Amriya Pharmaceuticals, Alexandria, Egypt.

⁵ To whom correspondence should be addressed (e-mail: hghandeh@rx.umaryland.edu).

ABBREVIATIONS: PEG, poly(ethylene glycol); PAMAM, poly(amidoamine) dendrimers; G, generation; FITC, fluorescein isothiocyanate; M_w , weight average molecular weight.

INTRODUCTION

The central component of most new drug delivery systems is a polymeric biomaterial. Among polymeric biomaterials that have been examined as drug carriers is a family of water-soluble cascade polymers named poly(amidoamine) (PAMAM) dendrimers. PAMAM dendrimers have a unique tree-like branching architecture that confers them a compact spherical shape in solution and a controlled incremental increase in size, molecular weight, and number of surface amine groups (Table 1 and Fig. 1) (1–4). The potential of PAMAM dendrimers in controlled drug delivery has been extensively investigated and arises from the high number of arms and surface amine groups that can be utilized to immobilize drugs, enzymes, antibodies, or other bioactive agents (5). Such conjugates provide a high density of biological agents in a compact system. In addition, PAMAM dendrimers have shown potential as oligonucleotide (6) and gene delivery systems (7–9), have been used to improve the solubility of sparingly soluble drugs such as piroxicam (10), and have increased the amount of therapeutic radionuclides delivered to cancer cells (11).

To reach the target site, polymeric drug delivery systems including PAMAM dendrimers often must extravasate from the microvasculature across the microvessels' endothelium into the surrounding interstitial tissue. The extravasation process of polymeric drug carriers influences the rate of drug delivery to the interstitial tissue, which is the site of action of most drugs. In this study, the extravasation of a series of PAMAM dendrimers across microvascular network endothelium is reported. The unique architecture of PAMAM dendrimers makes them suitable models for studying the influence of a controlled incremental increase in size, molecular weight, and number of amine surface groups on the microvascular extravasation of polymeric drug carriers. In an attempt to probe the influence of molecular geometry of polymeric drug carriers on their transvascular transport, the extravasation of linear poly(ethylene glycol) (PEG) molecules is also included and compared to its PAMAM dendrimer counterparts.

MATERIALS AND METHODS

Materials

Aqueous solutions of PAMAM dendrimers (G0–G4) were purchased from Dendritech, Inc. (Midland, MI). Fluorescein isothiocyanate (FITC) was purchased from Sigma-Aldrich Co. (St. Louis, MO). Superose 12 HR 10/30 column, Superose 12 preparative grade beads, and HR 16/50 column were purchased from Amersham Pharmacia Biotech (Piscataway, NJ). Sodium azide, sodium chloride, Tris (hydroxymethyl) aminomethane, and phosphate-buffered saline (PBS) chemicals were purchased from Fisher Scientific (Norcross, GA). Spectra/Por CE dialysis membranes of molecular weight cutoff 500 Da were purchased from VWR Scientific Products (Atlanta, GA). Linear amino-PEG of average molecular weight 6000 Da was purchased from Shearwater Polymers, Inc. (Huntsville, AL). HPLC grade solvents, acetone and acetonitrile were purchased from Sigma-Aldrich Co. Male golden Syrian hamsters were purchased from Harlan, Inc. (Indianapolis, IN).

Table 1. Relation Between Molecular Weight, Size, and Number of Surface Amine Groups of Polymeric Probes and Their Extravasation Time (τ)

Probe	Molecular weight (Da)	Diameter (\AA) ^a	Number of surface NH ₂ groups ^c	Extravasation time (s) ^d
G0	517 ^a	15	4 ^a	143.9 ± 11.9
G1	1430 ^a	22	8 ^a	166.1 ± 14.5
G2	3256 ^a	29	16 ^a	179.8 ± 18.8
G3	6909 ^a	36	32 ^a	203.8 ± 19.3
G4	14,215 ^a	45	64 ^a	422.7 ± 34.3
PEG	6000 ^b	N/A	1 ^b	453.9 ± 27.1

^a Reported by Tomalia *et al.* (4).

^b Reported by Shearwater Polymers, Inc. (Huntsville, AL).

^c Number of surface amine groups for unlabeled polymers.

^d Extravasation time (τ) is the average ± standard error of four examined fields in four hamsters per polymeric probe (i.e., total of 16 fields per probe).

Synthesis and Fractionation of Fluorescently Labeled Probes

Size Exclusion Chromatography of Unlabeled PAMAM Dendrimers. The polydispersity of PAMAM dendrimers was qualitatively studied by examining the elution profiles of their aqueous solutions through a Superose 12 HR 10/30 column. The mobile phase used was composed of (30:70 v/v) acetonitrile/Tris buffer (pH 8). The flow rate of the mobile phase was adjusted to 1 ml/min. The eluting molecules were detected using an UV detector at a fixed wave length ($\lambda = 280$ nm). All the PAMAM dendrimers under study (i.e., G0–G4) showed broad elution profiles that increased with the increase in generation number (i.e., with the increase in molecular weight and degree of branching).

Fluorescence Labeling of PAMAM Dendrimers and Amino-PEG. PAMAM dendrimers (G0–G4) and amino-PEG (M_w 6000 Da) were labeled using FITC following the method reported by Yu and Russo (12). PAMAM aqueous solutions were diluted with a dilution factor of 100 (v/v) in PBS of pH 7.4. PEG was dissolved in PBS of pH 7.4. The corresponding amount of FITC (i.e., polymer:FITC molar ratio = 1:1) was dissolved in acetone to give a solution of concentration <5 mg/ml and added to regular unlabeled PAMAM or PEG solutions, which were then allowed to stand overnight at room temperature with stirring.

Purification and Fractionation of Fluorescently Labeled Probes. Fluorescently labeled PAMAM and PEG solutions were dialyzed against deionized water. The dialyzed solutions were fractionated on a Superose 12 HR 16/50 preparative scale column using a Fast Protein Liquid Chromatography

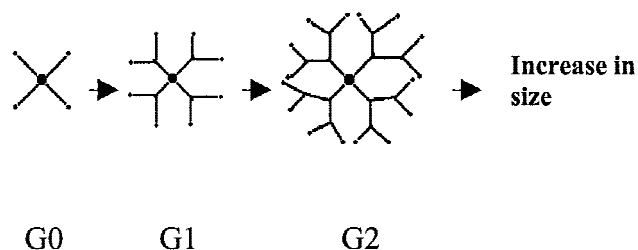


Fig. 1. Schematic drawing of G0, G1, and G2 of starburst dendrimers showing their tree-like branching architecture. The increase in generation number (G0, G1, G2, etc.) results in an incremental increase in size, molecular weight, and number of amine surface groups.

System (FPLC) (Amersham Pharmacia Biotech, Piscataway, NJ). The mobile phase was composed of (30:70 v/v) acetonitrile/Tris buffer (pH 8) and the flow rate was adjusted to 1 ml/min. Detection of eluting molecules was done using a UV detector at a fixed wavelength ($\lambda = 280$ nm). The fractions corresponding to the size and molecular weight of each probe were collected (Fig. 2). The collected fractions of each probe were dialyzed against deionized water to remove the mobile phase salts. The dialyzed solutions were subsequently lyophilized and stored at 4°C for the extravasation experiments.

In Vivo Extravasation of the Fluorescently Labeled Polymers *The Animal Model and Surgical Procedure.*

The cremaster muscle of male golden Syrian hamsters was used as an *in vivo* experimental model for this study. This preparation consists of a thin layer of muscle tissue that can be transilluminated and therefore is well suited for intravital microscopy. Details of the experimental techniques are published elsewhere (13) and will be briefly described here.

The animals used were at 7–8 weeks of age (90 ± 5.0 g, mean \pm SD). The surgical method was a modification of an open cremaster muscle preparation presented by Baez (14). Prior to the surgery, animals were anesthetized with an intraperitoneal (IP) injection consisting of 600 mg/kg of urethane and 90 mg/kg of α -chlorase. Body temperature was maintained at approximately 37°C by a silicone heating mat (Cole-Parmer, Chicago, IL). Animals were intubated, catheterized (left femoral vein), and placed on a surgical board where the right cremaster muscle was pinned as a flat sheet with minimal disruption to the tissue. Preparations were maintained viable at a temperature of $37 \pm 0.5^\circ\text{C}$ and superfused at a rate of 5 ml/min with a bicarbonate buffered salt solution equilibrated with 5% CO₂/95% N₂. After surgery the tissue was allowed to stabilize for 30 min before the fluorescently labeled polymer was administered as a single bolus dose and data collection was initiated. All protocols were approved by the Animal Care and Use Committee of the University of Tennessee Health Science Center, Memphis, and followed guidelines of the National Institutes of Health.

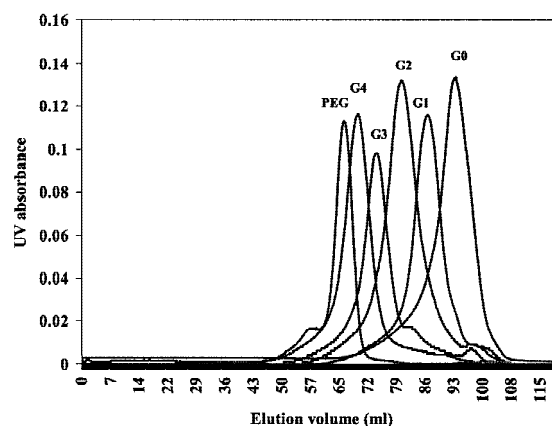


Fig. 2. Size exclusion chromatogram of the studied fluorescently labeled polymeric probes after fractionation. Size exclusion profile of the fluorescently labeled polymers on a Superose 12 HR preparative scale column (Amersham Pharmacia Biotech, Piscataway, NJ) using a mobile phase composed of 30:70 (v/v) acetonitrile/Tris buffer (pH 8) at a flow rate of 1 ml/min. Detection of eluting molecules was done using a UV detector at a fixed wavelength ($\lambda = 280$ nm).

Intravital Microscopy and SVHS Recordings. Microvascular networks were observed using intravital microscopy techniques. An industrial scale grade microscope (model MM-11, Nikon, Melville, NY) employing two camera assemblies and consisting of bright field (75 W xenon) and fluorescent (100 W mercury) light sources was used. With a 20xw objective lens, this assembly was used to obtain fluorescent images from which the microvascular extravasation of the probes into the interstitial tissue was estimated. Experiments were viewed on a video monitor (Panasonic WV-5410) and recorded on a SVHS VCR (JVC HR-54900U) for off-line analysis.

Data Collection and Analysis. Extravasation of the fluorescently labeled probes and measurement of the vessel diameter for all vessels within a network were done using a computerized video image analysis system (Metamorph Imaging System, Westchester, PA) in conjunction with a SVHS video recorder (Sony SV-9500MD). Direct measurements of vessel diameter were made off-line from SVHS videotapes

using an interactive routine developed within the Metamorph environment. The determination of the vessel type (i.e., venule or arteriole) was based on the blood flow direction and pattern. The extravasation measurements of the fluorescently labeled polymers were made from the fluorescent images. An image was acquired and the fluorescence intensities in selected areas in both a given vessel and its surrounding interstitial tissue in the field were measured. Data were collected for 30 min starting directly with the injection of the fluorescently labeled polymer via the femoral vein catheter. The tissue preparation was illuminated for 5 s every 30 s for 30 min. The change in the fluorescence intensity with respect to time in both the vessel and the tissue was measured and used as an index of the extravasation rate for each probe (Fig. 3).

Control Measures. As a control measure, light-induced quenching of the probe's fluorescence was quantified using two different concentrations of the fluorescently labeled probes (0.2 and 0.3 mg/ml) to represent the upper and lower expected concentrations of the probes in blood. These con-

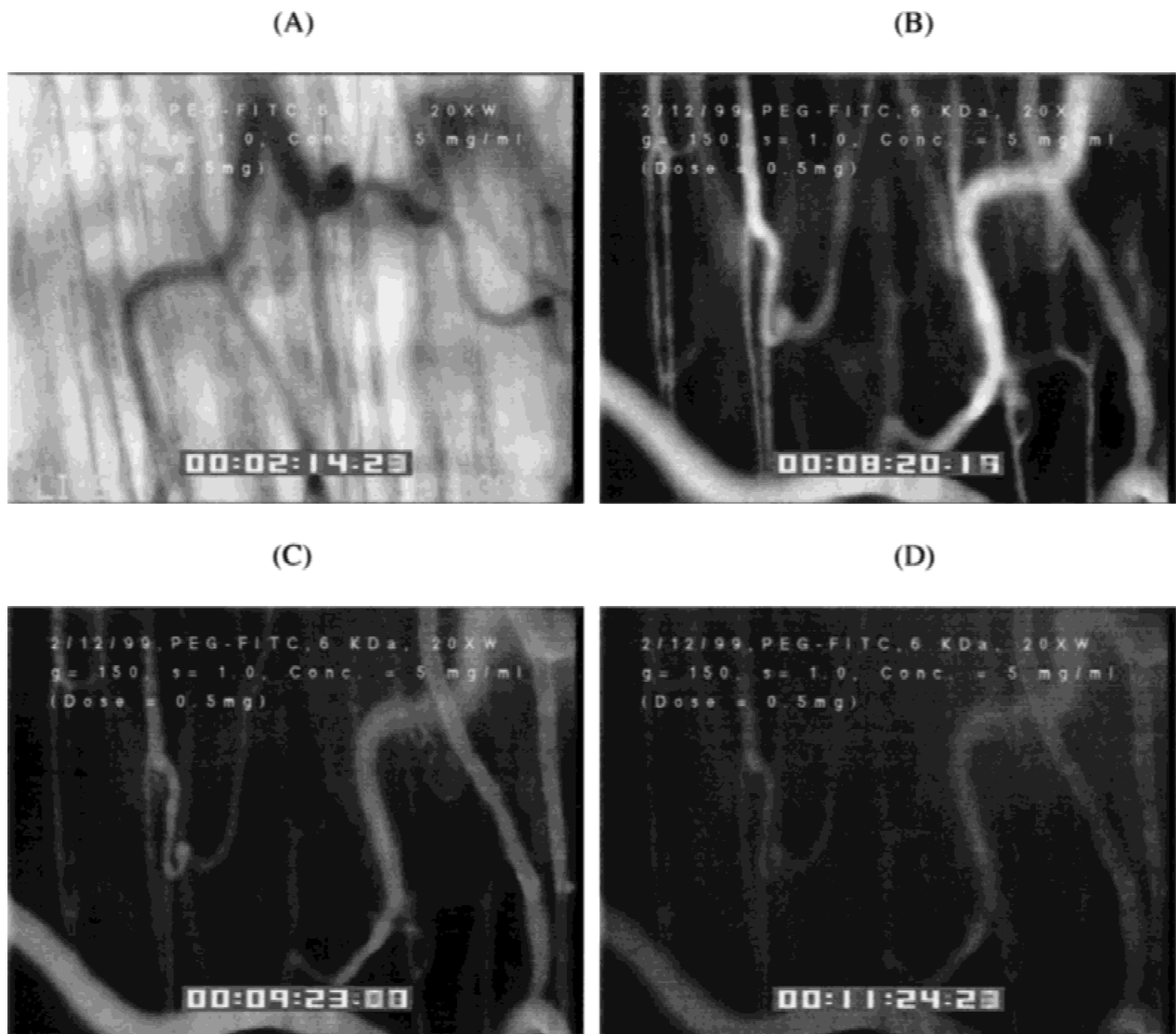


Fig. 3. Typical intravital microscopic images showing the extravasation of fluorescently labeled polymeric probes using an objective lens of magnification power 20xw: (A) Transilluminated image of the microvascular network *prior to the injection* of PEG-FITC; (B) fluorescent field image *directly after the injection* of PEG-FITC; (C) fluorescent field image *63 s after the injection* of PEG-FITC; (D) fluorescent field image *184 s after the injection* of PEG-FITC.

concentrations were calculated based on the fact that 1 mg of the probe was injected per hamster while the total blood volume per hamster is approximately 4–5 ml. Each probe was placed inside a separate polyethylene tube (PE60), which was positioned under the microscope and epiilluminated for 5 s every 30 s for 30 min. This was done to mimic the *in vivo* experimental conditions. Changes in fluorescence intensity during epiillumination in each tube were measured with respect to time and were used as an index of the probe's quenching. Our results indicated that light-induced quenching was negligible (i.e., in the range of 2%).

Another control measure was to consider the fluorescence-induced increase in microvascular permeability due to the photoactivation of the FITC conjugates. This was quantified using a photohemolysis assay described by Miller *et al.* (15,16). Hamster erythrocytes in *N*-(2-hydroxyethyl)piperazine-*N'*-ethanesulfonic acid (HEPES) buffer with 2.5% albumin (5% hematocrit) were incubated overnight with different fluorescently labeled probes (0.25 mg/ml) used in this study. The erythrocyte-probe mixture was placed in a hemocytometer (0.1-mm-deep hemocytometer, American Optical, Buffalo, NY) and was continuously epiilluminated for 10 min. The difference in light transmission through the mixture before and after the epiillumination period indicates the extent of erythrocytes' membrane disruption and similarly the endothelial cells' membrane disruption. This was used as an index of the FITC action on the endothelial cell membrane integrity and consequently on the microvascular permeability. For all erythrocyte-probe mixtures, there was less than 2% change in light transmission after a 10 min epiillumination period.

RESULTS

Size Exclusion Profiles of the Fluorescently Labeled Polymers

Fractionation of fluorescently labeled polymers was based on the principles of size exclusion chromatography, i.e., molecules with large hydrodynamic volumes elute earlier than those with smaller hydrodynamic volumes. The elution volumes of the fluorescently labeled probes were used as indicators of their relative sizes. As expected, the elution volumes of PAMAM dendrimers were in the order $G0 > G1 > G2 > G3 > G4$ (Fig. 2). The elution volume of PEG (M_w 6000 Da) was expected to be in the range between G2 (molecular weight 3256 Da) and G3 (molecular weight 6909 Da). However, PEG (M_w 6000 Da) eluted earlier than G4 (molecular weight 14,215 Da), which suggests that PEG has a larger hydrodynamic volume than PAMAM dendrimers (G0–G4).

Charge Distribution of Fluorescently Labeled Polymers at pH 7.4

PAMAM dendrimers have primary and tertiary amine groups, which differ in their pK_a values. Interior tertiary amine groups have a reported pK_a of 3.86, whereas the surface primary amine groups have a pK_a of 6.85 (4). The extent of ionization of the different amine groups of PAMAM dendrimers at pH 7.4 was estimated using Henderson-Hasselbalch equation:

$$pH = pK_a + \log \left[\frac{\text{base}}{\text{salt}} \right]$$

At pH 7.4, 22% of the surface primary amine groups are positively charged while the interior tertiary amine groups are almost uncharged (i.e., only 0.03% is positively charged). Linear amino-PEG (M_w 6000 Da) has only one terminal amine group that was consumed in covalent linkage to FITC molecules, which in turn rendered PEG chains uncharged at pH 7.4.

In Vivo Extravasation of the Fluorescently Labeled Polymers

Extravasation of the fluorescently labeled polymers is reported in terms of the extravasation time (τ). Extravasation time (τ) was arbitrarily determined to be the time needed for the fluorescence intensity in the interstitial tissue to reach 90% of the fluorescence intensity in the neighboring microvasculature. Extravasation time (τ) describes the rate of extravasation or transvascular transport of polymeric drug carriers across microvascular endothelium into the interstitial tissue. The reported extravasation time (τ), for each fluorescently labeled probe, is the average of 16 different examined fields (i.e., product of 4 different fields in 4 different hamsters). Extravasation of PAMAM dendrimers clearly showed size and molecular weight dependence. Increase in molecular weight of PAMAM dendrimers resulted in a corresponding exponential increase ($Y = 139.26 \times e^{7E - 05X}$, $r^2 = 0.9639$) in the extravasation time (τ) (Table 1 and Fig. 4). Similarly, the increase in size of PAMAM dendrimers resulted in a corresponding exponential increase ($Y = 78.74 \times E^{0.0327X}$, $r^2 = 0.8265$) in extravasation time (τ) (Table 1 and Fig. 5). The order of extravasation time (τ) of PAMAM dendrimers was $G0 < G1 < G2 < G3 < G4$ and covered the range 143.9–422.7 s (Figs. 4 and 5). On the basis of the molecular weight of PEG (M_w 6000 Da), its extravasation time (τ) was expected to be between the extravasation times of G2 (molecular weight 3256 Da) and G3 (molecular weight 6909 Da). However, extravasation time (τ) of PEG was longer than that of G4 (molecular weight 14,215 Da) (Table 1 and Fig. 4 and 6).

DISCUSSION

This research was designed to study the influence of a controlled incremental increase in size and molecular weight of PAMAM dendrimers, as model polymeric drug carriers, on their extravasation across microvascular network endothe-

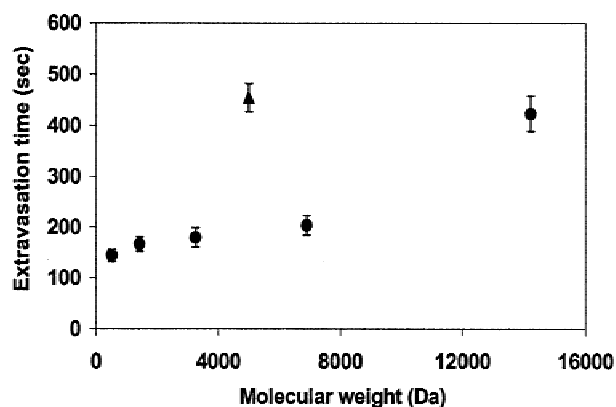


Fig. 4. The relation between extravasation time (τ) (s) and the molecular weight of the polymers. (●), PAMAM dendrimers; (▲), PEG.

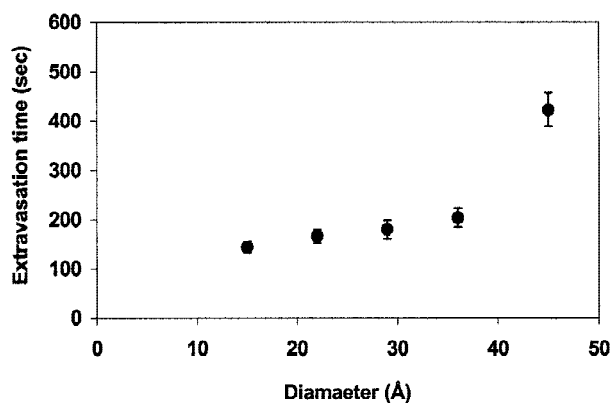


Fig. 5. The relation between the extravasation time (τ) (s) of PAMAM dendrimers and their corresponding diameters.

lium. Fluorescence labeling of PAMAM dendrimers and PEG using FITC was done to facilitate the detection and the visualization of the fluorescently labeled probes in biological matrices.

Careful fractionation of the labeled dendrimers was a necessary component of the reported studies because size exclusion profiles of the unlabeled dendrimers showed a broad molecular weight distribution that increased with the increase in generation number. Such polydisperse profiles may be explained by the defective (i.e., incomplete) branching during the dendrimers' synthesis, therefore resulting in a population of polydisperse polymers (4,17). Polydispersity of the studied probes could have compromised the accuracy by which extravasation across microvascular endothelium was measured due to the contributions of higher and lower molecular weight defective polymers. To avoid these contributions, fractionation of the probes under study was done with the collection of narrowly distributed polymers in order to minimize chances of error due to polydispersity of the polymers (Fig. 2).

The elution of linear PEG earlier than PAMAM dendrimers can be explained by the fact that PAMAM dendrimers exist in solution as compact spheres showing a controlled incremental increase in size, hydrodynamic volume, and molecular weight (4), whereas hydrated PEG chains acquire folded or random coiled conformation in solution (18). Such coiled conformation may have conferred linear PEG chains a larger hydrodynamic volume when compared to its dendritic counterparts, which, in turn, resulted in its earlier elution out of the size exclusion column (Fig. 6).

The observed order of extravasation of PAMAM dendrimers and linear PEG can be interpreted by considering the ultrastructure of the microvascular endothelium. Microvascular endothelium is lined with a negatively charged layer composed of sulfated glycosaminoglycan, known as the glycocalyx layer (19). Glycocalyx lines the luminal side of the endothelium and extends into the intercellular clefts. Plasma proteins are adsorbed to the glycocalyx, forming a "molecular filter" at the endothelial cell surface which adds to the properties of the glycocalyx layer as a barrier to the diffusion of macromolecules (19–21). In addition, investigations of the junctions' ultrastructure suggest that membranes of adjacent endothelial cells do not fuse but are separated by a space 4–8 nm wide (22–24). The glycocalyx layer together with the interendothe-

lial junctional strands control the size selectivity of the microvascular endothelium toward diffusing molecules such as PAMAM dendrimers and PEG molecules (19–23).

Size selectivity of microvascular endothelium toward water and hydrophilic solutes, such as PAMAM dendrimers and PEG molecules, is best explained by the "fiber-entrance junctional break" model. Such a model suggests that the endothelial pore size is not determined by the spacing between adjacent endothelial cells at the level of the tight junctions, but by the interfiber spacing in the fiber matrix at the entrance of the interendothelial clefts or fenestrations (21), as well as the length and frequency of the break or discontinuity in junctional strands (25).

Given the hydrophilic nature of PAMAM dendrimers and PEG molecules, it is likely that they cross the microvascular endothelium through the established pathways for transvascular transport of hydrophilic solutes. Given that the reported diameters of PAMAM dendrimers are in the range of 15–45 Å (4), it appears that they cross the microvascular endothelium by diffusing through the small endothelial pores with reported radii of 4–5 nm due to their relative abundance in microvessel walls compared to larger pores. Diffusion of hydrophilic solutes, including PAMAM dendrimers and PEG, follows the concept of "restricted diffusion." Restricted diffusion of hydrophilic solutes across membranes can be explained because as the size of the diffusing molecule increases, the exerted viscous drag on it together with its degree of exclusion from the membrane pores increase (26). Relevant to the probes used in our study, as the molecular diameter of PAMAM dendrimers increased, the degree of their exclusion from the endothelial pores also increased. This explains the increase in the extravasation time (τ) as the size of PAMAM dendrimers increased from 15 to 45 Å. It also appears that the coiled conformation of hydrated PEG chains conferred them a larger hydrodynamic volume than any of the PAMAM dendrimers. As a result, PEG took a longer time to extravasate across the microvessel endothelium into the interstitial tissue than any of the dendritic polymers.

It is known that the polyanionic nature of the glycocalyx layer lining the luminal endothelial surfaces, the walls of endothelial pores, and the endothelial vesicles influences transvascular transport of charged molecules (27). It was shown

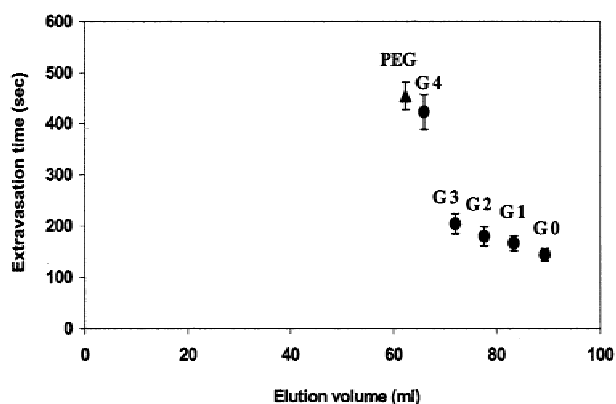


Fig. 6. The relation between extravasation time (τ) (s) and the elution volume of polymers on a Superose 12 HR 16/50 preparative scale column (Amersham Pharmacia Biotech) following the experimental conditions reported in the experimental methodology section. (●), PAMAM dendrimers; (▲), PEG.

that solutes carrying a net positive charge accumulate in the tissue more readily than similar-sized solutes carrying a net negative charge (27). Considering the anionic nature of the endothelial glycocalyx, electrophysiological interactions between the studied polymers and the endothelial membrane may have contributed to the observed extravasation of PEG and PAMAM dendrimers. On the basis of the calculations of the charge of PAMAM dendrimers using the Henderson-Hasselbalch equation, PAMAM dendrimers carry a partial positive charge (i.e., 22% of the primary surface amine groups) at pH 7.4, whereas PEG molecules are neutral. Partial positive charge of PAMAM dendrimers may have favored their electrophysiological interaction with the polyanionic glycocalyx layer lining the microvascular endothelium that may have resulted in fast extravasation across the microvasculature and accumulation in the interstitial tissue. However, this does not apply for PEG chains. At physiologic pH, PEG molecules were neutral.

It appears that the observed difference in the extravasation time (τ) between PAMAM dendrimers and PEG is due to a combination of both steric and electrophysiological factors based on the inherited molecular geometry and charge properties of the studied probes.

We acknowledge that utilizing the cremaster muscle preparation, as an *in vivo* model, for extravasation experiments has limitations. One such limitation is the possible uptake of the studied polymers by different organs in the body, in addition to possible interactions of PAMAM dendrimers and/or PEG with plasma components. Therefore, careful *in vitro* permeability studies of polymeric probes across endothelial cell monolayers are the next logical step to elucidate the factors that influence microvascular permeability of polymeric drug carriers.

In conclusion, extravasation of PAMAM dendrimers, as model polymeric drug carriers, showed size and molecular weight dependence. An increase in size and/or molecular weight of PAMAM dendrimers resulted in a corresponding exponential increase in the extravasation time (τ). Results suggest that in addition to size and molecular weight, charge and molecular geometry of polymeric drug carriers also influence their microvascular extravasation across the endothelial barrier. Such a systematic approach in characterizing the influence of the physicochemical properties of polymeric drug carriers on their transvascular transport will aid in the design of novel polymeric biomaterials with controlled extravasation profiles.

REFERENCES

1. D. A. Tomalia. StarburstTM/cascade dendrimers: fundamental building blocks for a new nanoscopic chemistry set. *Aldrichim. Acta.* **26**:91-101 (1993).
2. D. A. Tomalia, H. Baker, J. Dewald, M. Hall, G. Kallos, S. Martin, J. Roeck, J. Ryder, and P. Smith. Dendritic macromolecules: synthesis of starburst dendrimers. *Macromolecules* **19**:2466-2468 (1986).
3. D. A. Tomalia, H. Baker, J. Dewald, M. Hall, G. Kallos, S. Martin, J. Roeck, J. Ryder, and P. Smith. A new class of polymers: starburst-dendritic macromolecules. *Polymer J.* **17**:117-132 (1985).
4. D. A. Tomalia, A. M. Naylor, and W. A. Goddard, III. Starburst dendrimers: molecular-level control of size, shape, surface chemistry, topology, and flexibility from atoms to macroscopic matter. *Angew. Chem., Int. Ed. Engl.* **29**:138-175 (1990).
5. N. A. Peppas. Star polymers and dendrimers: prospects of their use in drug delivery and pharmaceutical applications. *Controlled Release Soc. Newsl.* **12**:12-13 (1995).
6. R. Delong, K. Stephenson, T. L. M. Fisher, S. Alahari, A. Noltling, and R. L. Juliano. Characterization of complexes of oligonucleotides with polyamidoamine starburst dendrimers and effects on intracellular delivery. *J. Pharm. Sci.* **86**:762-764 (1997).
7. J. Haensler and F. C. Szoka. Polyamidoamine cascade polymers mediate efficient transfection of cells in culture. *Bioconjugate Chem.* **4**:372-379 (1993).
8. M. X. Tang, C. T. Redemann, and F. C. Szoka. In vitro gene delivery by degraded polyamidamine dendrimers. *Bioconjugate Chem.* **7**:703-714 (1996).
9. M. X. Tang and F. C. Szoka. The influence of polymer structure on the interactions of cationic polymers with DNA and morphology of the resulting complexes. *Gene Ther.* **4**:823-832 (1997).
10. R. Wiwattanapatapee, R. D. Jee, and R. Duncan. PAMAM dendrimers as a potential oral drug delivery system: Dendrimer complexes with piroxicam. In *Controlled Release of Bioactive Materials*, Boston, MA, 1999, pp. 145-146.
11. D. S. Wilbur, P. M. Pathare, D. K. Hamlin, K. R. Buhler, and R. L. Vessella. Biotin reagents for antibody pretargeting. 3. Synthesis, radioiodination, and evaluation of biotinylated starburst dendrimers. *Bioconjugate Chem.* **9**:813-825 (1998).
12. K. Yu and P. S. Russo. Light scattering and fluorescence photobleaching recovery study of poly(amidoamine) cascade polymers in aqueous solution. *J. Polym. Sci., Polym. Phys. Ed.* **34**:1467-1475 (1996).
13. N. M. Roth and M. F. Kiani. A "Geographic Information Systems" based technique for the study of microvascular networks. *Ann. Biomed. Eng.* **27**:42-47 (1999).
14. S. Baez. An open cremaster muscle preparation for the study of blood vessels by in vivo microscopy. *Microvasc. Res.* **5**:384-394 (1973).
15. F. N. Miller, G. J. Tangelder, D. W. Slaaf, and R. S. Reneman. Quantitation of erythrocyte photohemolysis by light microscopy. *Blood Cells* **17**:567-579 (1991).
16. F. N. Miller, D. E. Sims, D. A. Schuschke, and D. L. Abney. Differentiation of light-dye effects in the microcirculation. *Microvasc. Res.* **44**:166-184 (1992).
17. P. G. deGennes and H. J. Hervet. Statistics of "Starburst" polymers. *J. Phys. Lett. (Paris)* **44**:L351-L360 (1983).
18. M. G. Davidson and W. M. Deen. Hindered diffusion of water-soluble macromolecules in membranes. *Macromolecules* **21**:3474-3481 (1988).
19. R. H. Adamson and G. Clough. Plasma proteins modify the endothelial cell glycocalyx of frog mesenteric microvessels. *J. Physiol. (London)* **445**:473-486 (1992).
20. G. Clough and C. C. Michel. Quantitative comparisons of hydraulic permeability and endothelial intercellular cleft dimensions in single frog capillaries. *J. Physiol. (London)* **405**:563-576 (1988).
21. F. E. Curry and C. C. Michel. A fiber matrix model of capillary permeability. *Microvasc. Res.* **20**:96-99 (1980).
22. M. Simionescu, N. Simionescu, and G. E. Palade. Structural basis of permeability in sequential segments of the microvasculature of the diaphragm. II. Pathways followed by microperoxidase across the endothelium. *Microvasc. Res.* **15**:17-36 (1978).
23. M. Simionescu and N. Simionescu. Ultrastructure of microvessel wall: functional correlations. In E. M. Renkin and C. Michel (eds.), *Handbook of Physiology*, American Physiological Society, Bethesda, 1984, pp. 41-101.
24. S. L. Wissig. Identification of the small pore in muscle capillaries. *Acta Physiol. Scand.* **463**(Suppl.):33-44 (1979).
25. R. H. Adamson and C. C. Michel. Pathways through the intercellular clefts of frog mesenteric capillaries. *J. Physiol. (London)* **466**:303-327 (1993).
26. J. R. Pappenheimer, E. M. Renkin, and J. M. Borrero. Filtration, diffusion and molecular sieving through peripheral capillary membranes. A contribution to the pore theory of capillary permeability. *Am. J. Physiol.* **167**:13-46 (1951).
27. F. E. Curry, J. C. Rutledge, and J. F. Lenz. Modulation of microvessel wall charge by plasma glycoprotein orosomucoid. *Am. J. Physiol.* **257**:H1354-H1359 (1989).